Available online at www.sciencedirect.com

ScienceDirect

Procedia Engineering 149 (2016) 62 – 66

Procedia Engineering

www.elsevier.com/locate/procedia

International Conference on Manufacturing Engineering and Materials, ICMEM2016, 6-10 June 2016, Novy Smokoves, Slovakia

Friction Stir Welding Process of Aluminum-Lithium Alloy 2195

Ho-Sung Lee[a,b]*, Jong-Hoon Yoon[a], Joon-Tae Yoo[a] and Kookil No[b]

[a]*Korea Aerospace Research Institute 169-84 Gwahak-ro, Yuseong-gu, Daejeon, 34133, Korea*
[b]*Department of Aerospace System Engineering*
University of Science & Technology, 217 Gajung-dong Yuseong-gu, Daejeon 34113, Korea

Abstract

Friction stir welding is solid state welding and involves heating the metal with a suitable amount of pressure so that homogeneous and complete microstructural welding is possible without melting of the parts to be joined. The process uses a rotating tool with a profiled pin that penetrates the parts to be joined; the tool then starts to travel along the join line. By keeping the tool rotating and moving it along the join line to be welded, the softened material due to the frictional heat is stirred and mixed together by the rotating pin forming a weld in solid state without melting. Frictional heat generated by rotation of the tool due to the high compressive pressure and shearing action of the shoulder along the joint line causes a softened zone of material without melting. Localized severe deformation around the tool results in refinement of the microstructure and the material flow produces coalescence and formation of a weld. FSW provides superior welding over conventional fusion welding and is preferred for joining of Al-Li alloys. The present work is to investigate was to study the effect of friction stir welding parameters on mechanical and microstructural properties of AA2195-T0 and T8. Since FSW is both a deformation and a thermal process, temperature distribution during FSW is measured. The microstructure and mechanical properties of welded joint were investigated for different friction stir welding conditions. This paper describes the results of an experimental study to investigate the mechanical and microstructure evolution of AA2195 friction stir welded joint. The optimum welding condition is also provided for different heat treated AA2195 alloys.

Peer-review under responsibility of the organizing committee of ICMEM 2016

Keywords: Friction Stir Welding; Process Parameters; Mechanical Properties; Al-Li alloy

1. Introduction

It is well known that the addition of Li to aluminum alloys offers an attractive combination of low density and high modulus, which are useful for lightweight structures of aerospace vehicles. The low density and good mechanical properties of AA2195 make them successfully used in Space Shuttle super lightweight tank(SLWT) since the first successful flight in 1998. By replacing AA2219 which was conventionally used to build the external tank of Space Shuttle with AA2195 for the super lightweight external tank, the mass reduction of over 10% and increasing the payload capability were achieved [1,2]. However, the hygroscopic property of element Li causes porosity, cracking [3,4] and low joint efficiency. It is known that these alloys exhibit an unusual fusion boundary cracking phenomenon that is associated with an equiaxed grain zone that forms via a solidification mechanism in alloys containing precipitates of Li and Zr. This is because the combination of Li and Cu in the

* Corresponding author. Tel.: +82-42-860-2512
*E-mail address:hslee@*kari.re.kr
* Corresponding author. Tel.: +0-000-000-0000 ; fax: +0-000-000-0000.
E-mail address: author@institute.xxx

Peer-review under responsibility of the organizing committee of ICMEM 2016
doi:10.1016/j.proeng.2016.06.639

interface liquid lowers the eutectic temperature of the liquid and is responsible for the hot cracking problem [5]. Therefore, friction stir welding in solid state is preferred to avoid solidification cracking for joining of this alloy.

Friction Stir Welding (FSW) is a solid-state welding process, invented at the Welding Institute (TWI) in 1991 [6]. Joining takes place by means of a non-consumable rotating tool with a threaded pin to provide a combination of frictional heating by the tool shoulder, and stirring of the soft material by the pin along the joint line. It is important to avoid overheating since the temperature must be maintained to be below the solidus of the equilibrium phase diagram for the materials being joined. The main advantage is its ability to join metals without melting precludes the risk of traditional defects found in fusion welds such as liquidation cracking, solidification cracking, or oxide formation. Frictional heat generated by rotation of the tool due to the high normal pressure and shearing action of the shoulder along the joint line causes a softened zone of material without melting. This softened material cannot escape outside as it is under constrained extrusion by the tool shoulder. As the tool travels along the joint line, material is moved around the tool probe between the retreating side of the tool and the surrounding non-deformed material. The mixed and extruded material is deposited to form a mechanically mixed joint in solid state behind the tool [7]. After cooling, a solid phase bond is created in microstructure of metal that has been stirred and mixed together. This process requires low energy input and joins materials without consumable filler metals, sparks, fumes, or shielding gas, so it is a kind of green technology. It is energy efficient and produces reliable products with automated process and improved productivity [8]. In addition, in most cases the localized heat during friction welding results in a refined microstructure, which can provide improved strength relative to the parent material. Key process parameters include travel speed, rotational speed, normal compressive load, and fixture geometry. The details of the tool geometry are crucial for determining optimum condition and usually are proprietary.

The purpose of the current study was to study the friction stir welding process on mechanical and microstructural properties of Aluminum alloy 2195-T0 and T8. Since FSW is both a deformation and a thermal process, microstructural evolution during FSW is evaluated. The microstructure and mechanical properties of weldments were investigated for different welding conditions so that the optimum welding condition is determined for different heat treated alloys.

2. Experimental

The material used for this study is obtained from Constellium Global Aerospace, France. Two plates were butt-joined by friction stir welding apparatus as shown in Figure 1(a) and the welding direction was parallel to rolling direction with coupons of 300mm in length and 100mm in width. The thickness of the plate is 7.6 mm. The range of welding parameter is four rotation speeds (350, 400, 600 and 800 rpm) and five travel speeds (120, 180, 240, 300, and 360 mm/min). After welding, all of the specimens were inspected by x-ray radiography and one with defects are discarded. For optical microstructure, the specimens were etched with Graff-Sargent solution followed by Keller's solution. The cross-sectional specimen is prepared and the location of microstructural observation is shown in Figure 1(b) and (c). During welding, temperature distribution of welding area was monitored with 10 K-type thermocouples which were set on the surface of the plates on a line 100 mm distant from the weld-start point to measure the temperature distribution. There are 3 thermocouples on the advancing side located at 100mm from the start of welding and each 3 thermocouples are attached on advancing side and retreating side located at another 100mm. The location of temperature measurement and gage numbering is shown in Figure 1(d). Tensile specimens with 200 mm long and 12.8 mm wide gauge part were cut along the welded joints and tested at room temperature using a 100 KN MTS 810 testing machine with a crosshead speed of 2.0 mm/min. Micro-hardness of nugget region is measured using Future-Tech FM800. Cross-section of the nugget is scaled with 2 mm distance and depths from surface are 1.3 mm, 3.8 mm and 6.3 mm. Microstructures were examined by optical microscopy (Metallux 3, Leica Microsystems) and transmission electron diffraction microscopy (Titan G2 Double Cs corrected TEM, Philips/FEI) with an acceleration voltage of 200~300 kV. Composition was determined by energy-dispersive spectroscopy (EDS), electron energy loss spectroscopy (EELS) and scanning TEM-high angle annular dark field (STEM-HAADF) in the TEM. Samples for the TEM observation were prepared on Molybdenum-grid by a focused ion beam (FIB)-SEM hybrid system equipped with a Ga+ focused ion beam (FIB) column (FIB; SMI3050SE, SII Nanotechnology Inc.).

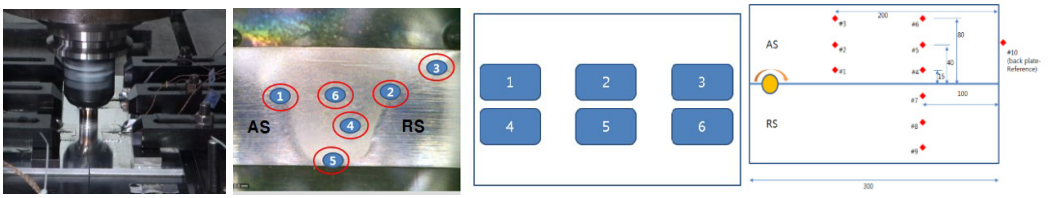

(a) (b) (c) (d)

Fig. 1. (a) Photograph of FSW process, (b) typical cross-sectional view of FSW specimen, (c) location of microstructure observation, and (d) layout of thermocouple location for temperature measurement

3. Results and Discussion

Figure 2 shows metallographic microstructure of AA2195-T0 and AA2195-T8 with some of precipitates. Precipitates are found at the grain boundaries and inside grain for AA2195-T8 and grain boundaries are not clearly visible for AA2195-T0. The precipitates are easy to nucleate at the gain boundaries because the high dislocation density is suitable for the diffusion of the solute elements at the grain boundaries. Furthermore, their size was ranged from nano-scale to 10 μm. On the other hand, average size of Al grains in a longitudinal surface (Figure 1(c)) was about 20μm, estimated by using linear intercept method. In contrast, that of Al grains in a cross-sectional surface (Fig. 5(d)) was assessed as 9μm. Since it is very hard to identify each precipitates, the STEM-HAADF micrographs and EELS results are analysed. The phase #3 in Figure 3(a) and (b) showed much contents of Zr while few contents of Cu were found. This result indicated that there existed ß' (Al_3Zr) phase. This phase is known to play a key role for hardening in AA2195 [9]. The phase #4, a needle-like phase of AA2195-T8 in Figure 3(b) showed Al–Cu–Li contents in EDS and EELS results. With the morphology and composition, this phase was T1 phase. This phase is responsible for high strength of AA2195-T8.

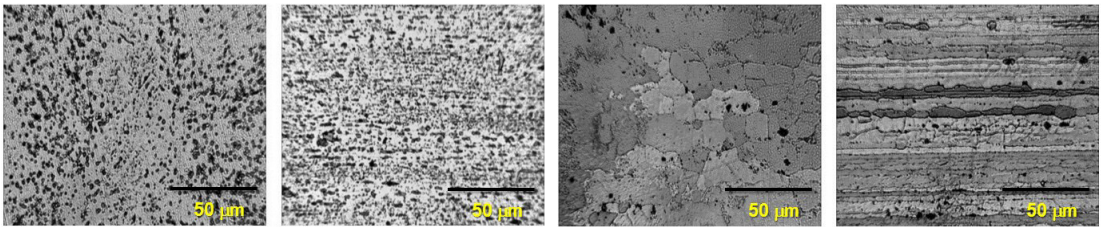

(a) (b) (c) (d)

Fig. 2. Metallographs of (a) longitudinal, (b) cross-sectional view of AA2195-T0, and (c) longitudinal, (d) cross-sectional view of AA2195-T8

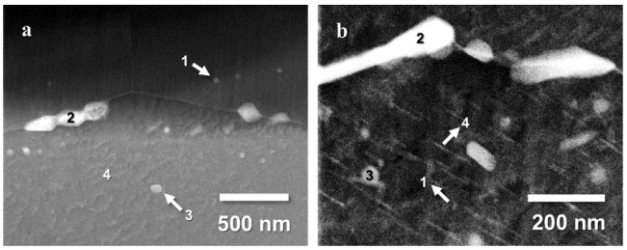

Fig. 3. Scanning TEM-HAADF micrographs of (a) AA2195-T0 and (b) AA2195-T8

Since the temperature distribution during FSW process influences the integrity of weld, the temperature profile is measured at different locations. Figure 4 shown result of temperature measurement at locations from Figure 1(d) for AA2195-T0 specimen welded with 600 RPM and 300 mm/min condition. One plate where the direction of rotation is the same as that of welding is called the advancing side (AS), with the other plate where tool rotation opposes the traversing direction, is designated as being the retreating side (RS). At this condition, the temperatures of advancing side at #4 increased to 207℃, while the maximum temperature of retreating side at #7 was 203℃. The temperature in advancing side is slightly higher than in retreating side. Generally it is known that the temperature in advancing side is higher than retreating side, since material flow around tool is moving from advancing side to retreating side additional to friction heat under the shoulder that gives higher temperature [10]. This is confirmed by the micro-hardness measurement of the nugget zone in this study.

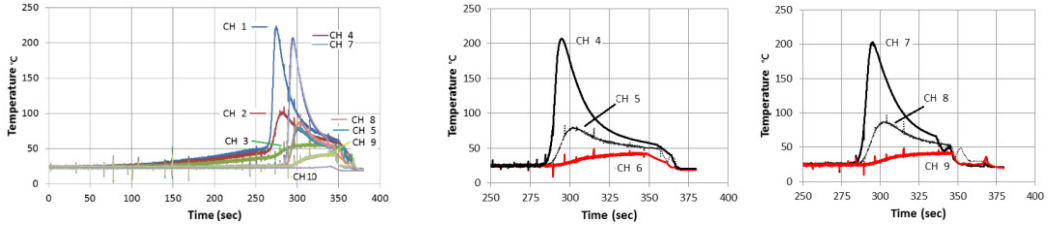

Fig. 4. Result of temperature measurement at different locations from Figure 1(d), measured during friction welding with 600 RPM and 300 mm/min condition

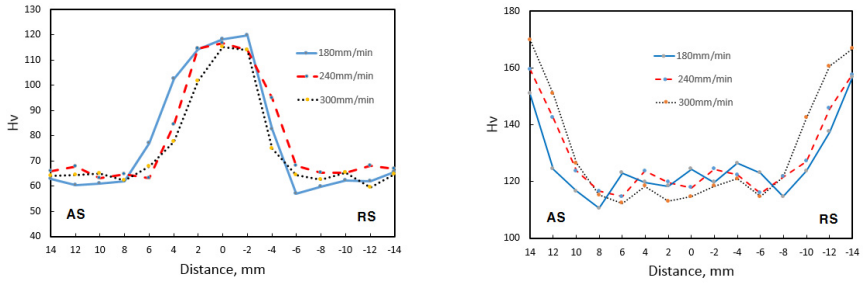

(a) (b)

Fig. 5. Result of micro-hardness measurement in nugget zone welded with 600rpm of (a) AA2195-T0 and (b) AA2195-T8

Figure 5 shows results of micro-hardness measurements for the friction stir welded at 600 RPM with different traveling speed for AA2195-T0 and AA2195-T8. The micro-hardness is measured at 3.87 mm from the surface and at every 2 mm distance. It is shown that hardness values are closely connected with the nature of the process experienced by the zones. The base hardness for AA2195-T0 is 63.7 Hv. The hardness of the nugget zone is found to be higher than that of the matrix due to the grain refinement during welding and cooling. The highest hardness of 124.3 Hv was obtained for the specimen welded at 300 mm/min and this is because of the fast cooling for this traveling speed. It is interesting to note the general trend of higher hardness for the measurements of retreating side comparing to advancing side. This can be also explained since materials on advancing side is exposure to higher temperature than materials on retreating side. The low hardness in the welded zone of AA2195-T8 is related to the dissolution and coarsening of precipitates in the advancing side and retreating side. The nominal hardness is 167 Hv for AA2195-T8. It shows the minimum micro-hardness value appears at the both end of TMAZ (Thermomechanically Affected Zone) and HAZ (Heat Affected Zone) for the specimen welded with 180 mm/min. This is due to the grain growth from long exposure time to frictional heat with slow the traveling speed and high frictional force at the interface. The minimum hardness on AS is 110 Hv, while as one on RS is 118 Hv, which supports the previous argument of the higher temperature on AS.

Figure 6 shows microstructure of friction stir welded AA2195 at 600rpm and300mm/min condition in each region identified in Figure 1(b) and 1(c). It has shown the boundary between TMAZ and nugget in the advancing side and dynamic recrystallization has taken placed in this region. Material in the stirred zone experience sufficient deformation and heat input which cause the complete dynamic recrystallization. In this condition, there is no welding defect detected. The material located at the advancing side is mainly influenced by the friction from shoulder and pin, while at the retreating side, the dominating effects are extrusion and backfill from the advancing side and the shoulder.

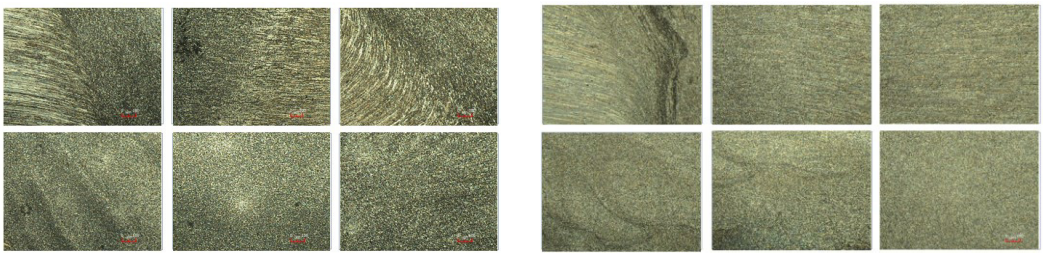

(a) (b)

Fig. 6. Result of macroscopic cross-sectional view of welded region of (a) AA2195-T0 and (b) AA2195-T8 with 600 RPM and 300 mm/min condition.

In order to study the effect of surface oxide on the welding integrity, the surface of the plate is machined to remove the surface oxide. The presence of oxide is known to be detrimental since it may be mixed in stirred zone. The thickness of the plate is 7.2 mm after removing surface oxide. Result of tensile test is shown in Figure 7 for (a) non-treatment and (b) without oxides. Tensile strength of the base material is 552 MPa. The increased properties are highlighted with bold in Figure 7(b). In this study, it is shown that the effect of removing oxide is effective on relatively low rotating speed condition of 300 and 400 rpm. This is due to the fact that the oxide film is easily broken down at higher rotating condition so that the presence of oxide does not effectively decrease the mechanical properties. By removing the surface oxide, it is possible to increase the strength by 15 MPa and the elongation by about 40% at rotating speed condition of 300 and 400 rpm. At rotating speed condition of over 600 rpm, some of oxide surface is acceptable since it does minimally influential to tensile strength and elongation. However, the presence of surface oxides on fatigue strength may show negative effects with formation of oxides bands [11].

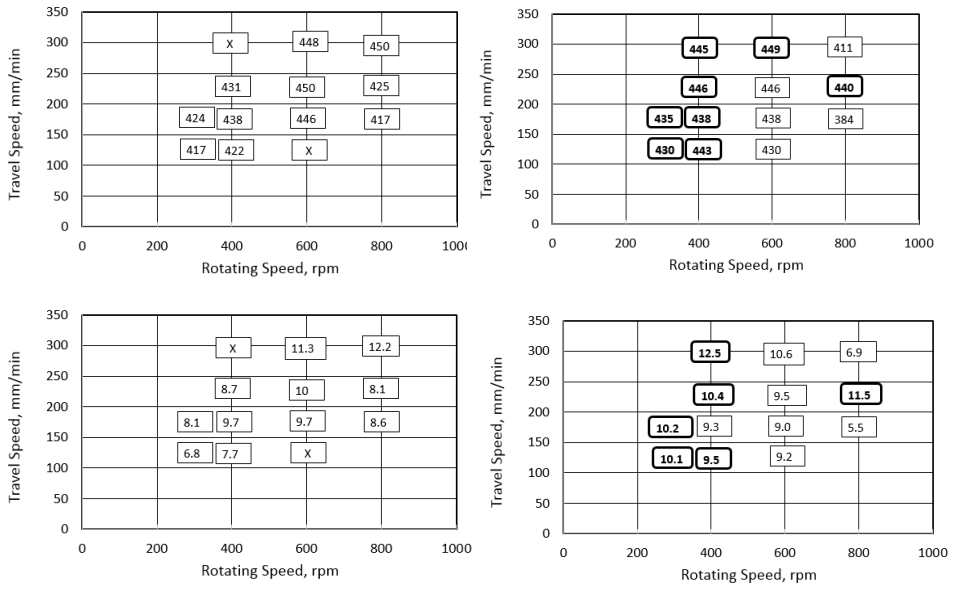

(a) (b)

Fig. 7. Comparison of tensile strength and elongation between (a) specimen welded with non-treatment, and (b) specimens without oxide at different welding parameters of AA2195-T8 (unit: MPa, %)

4. Conclusion

In this research, FSW butt jointed AA2195 specimens were tested. The microstructure was characterized with electron microscopy and during welding, surface temperatures were measured. It is shown that the temperature in advancing side is higher than retreating side which supports the results of micro-hardness profile at nugget zone. For AA2195-T0, The weld zone can exhibit higher micro-hardness than parent material due to grain recrystallization and the hardness profile inside of the nugget depends on the cooling rate. For AA2195-T8, low hardness around the nugget zone is related to the dissolution and coarsening of precipitates at HAZ in the advancing side and/or retreating side. It shows the minimum micro-hardness value appears at the location just adjacent to tool tip near HAZ interface. The effect of surface oxide on the tensile strength of joint is investigated by comparing to specimen without surface oxide. It is shown that the effect of removing oxide is effective on relatively low rotating speed condition of 300 and 400 rpm, while as little influence to specimens welded higher rotating speed in this study. Friction stir welding process map of this alloy represents the strength at each process parameters, which are rotating and traveling speeds.

References

[1] Davis, D., and McArthur, J., NASA Ares I Crew Launch Vehicle Upper Stage Overview, in: 44th AIAA/ASME/SAE/ASEE Joint Propulsion Conference & Exhibit, Connecticut, CT, USA, July 21.23 2008.
[2] Adams, G., Pareti, P., Thompson, J., and Lawless, K., AEROMAT 2001, June 11-14, 2001, Los Ang3les, CA., U.S.A.
[3] NASA Facts, Super Lightweight External Tank, FS-2005-04-025-MSFC, April 2005.
[4] Vickers, J. H., Fikes, J., Jackson, J. R., Johnson, T. F., Sutter, J. K., and Martin, R. A., “NASA Composite Cryotank Technology Demonstration: Overview”, SAMPE 2012 Conference, Baltimore, MD, 2012.
[5] Thompson, R. G., Analysis of weld hot cracks in Al-Li alloy 2195. In: Aluminum-Lithium Alloys for Aerospace Applications Wrokshop, NASA CP 3287, p. 246-263.
[6] Thomas, W. M., Nicholas, E. D., Needham, J. C., Nurch, M. G., Temple-Smith, P., and Dawes, C., "Patents on Friction Stir Butt Welding," International: PCT/GB92/02203; British: 9125978.8; USA: 5460317., p. 1991-1995.
[7] Mishra, R. S., Mahoney, M. W., McFadden, S. X., Mara, N. A., and Mukherjee, A. K., “High strain rate superplasticity in a friction stir processed 7075 al alloy,” Scripta Materialia, 2000;42:163-169.
[8] Burford, D., “Advances in Friction Stir Welding for Aerospace Applications”, 6th AIAA Aviation Technology, Integration and Operations Conference, September 25-27, 2006, Wichita, Kansas, U.S.
[9] Kumar, K., Brown, S., and Pickens, J., Microstructural evolution during aging of an Al-Cu-Li-Ag-Mg-Zr alloy, Acta Materialia, 1996;44:1899-1915.
[10] Muhsin, J. J., Moneer, H. T., and Muhammed, A. M., Effect of friction stir welding parameters (rotation and transverse) speed on the transient temperature distribution in friction stir welding of AA 7020-T53, Asian Research Publishing Network Journal of Engineering and Applied Sciences, 2012;7:436-446.
[11] Yang, S., Di, X., B., Luan, The influence of zigzag curve defect on the fatigue properties of friction stir welds in 7075-T6 Al alloy, Mater. Chem. Phys. 2007;104:244-248.